

# Crystallographic Design of Intercalation Materials

**Ananya Renuka Balakrishna**

Aerospace and Mechanical Engineering,  
University of Southern California,  
Los Angeles, CA 90089  
e-mail: renukaba@usc.edu

*Intercalation materials are promising candidates for reversible energy storage and are, for example, used as lithium-battery electrodes, hydrogen-storage compounds, and electrochromic materials. An important issue preventing the more widespread use of these materials is that they undergo structural transformations (of up to ~ 10% lattice strains) during intercalation, which expand the material, nucleate microcracks, and, ultimately, lead to material failure. Besides the structural transformation of lattices, the crystallographic texture of the intercalation material plays a key role in governing ion-transport properties, generating phase separation microstructures, and elastically interacting with crystal defects. In this review, I provide an overview of how the structural transformation of lattices, phase transformation microstructures, and crystallographic defects affect the chemo-mechanical properties of intercalation materials. In each section, I identify the key challenges and opportunities to crystallographically design intercalation compounds to improve their properties and lifespans. I predominantly cite examples from the literature of intercalation cathodes used in rechargeable batteries, however, the identified challenges and opportunities are transferable to a broader range of intercalation compounds.*

[DOI: 10.1115/1.4054858]

*Keywords:* intercalation materials, rechargeable batteries, phase transformations, crystallographic texture

## Introduction

Intercalation is the reversible insertion of active ions (or molecules) into a materials' lattice structure. This reversible insertion is often accompanied by a simultaneous change to the host materials' lattice structure and/or its physical properties (i.e., optical, thermal, electronic) [1]. This intrinsic coupling between ionic (or molecular) insertion and physical properties makes intercalation materials well-suited for next-generation applications, such as electrodes in lithium batteries [2], electrochromic materials in smart windows [3,4], and ion-exchange membranes in water desalination devices [5]. Despite the technological relevance of intercalation materials, their widespread use is plagued by chemo-mechanical challenges that limit material performance and lifespans [6–8].

The chemo-mechanical challenges in intercalation materials are closely associated with their crystallographic texture [7,9]. Inserting active ions into an intercalation material typically induces an abrupt change to its lattice parameters. This structural transformation of lattices—a characteristic feature of first-order phase transformation materials—induces macroscopic volume changes and generates lattice misfit strains in the material [8,10–12]. With repeated intercalation, these volume changes and internal stresses weaken the structural integrity of the material and shorten its lifespan [13]. In addition to the structural transformation of individual lattices, the crystallographic texture of the intercalation material plays a dominant role in governing ion-transport properties [7]. For example, intercalating ions in  $\text{LiCoO}_2$  (a commonly used cathode) preferentially diffuse parallel to the (001) crystallographic planes. This preferential diffusion constrains ion migration to specific crystallographic channels and thus limits rapid charge/discharge properties [14,15]. The presence of crystal defects, such as grain boundaries and edge dislocations, further affects ion diffusion pathways [16] and contributes to the irreversible cycling of intercalation compounds [17]. This interplay between the crystallographic texture and material properties leads us to a central question: Can we design the crystallographic texture of intercalation materials to improve their performance and lifespan?

Take shape-memory alloys—another family of phase transformation materials—which share commonalities with structural transformations in intercalation materials. For example, the Ti–Ni–Cu shape-memory alloy is accompanied by ~8% lattice strains during phase transformation, which is comparable to lattice strains in common intercalation materials. This large transformation strain contributes to material fatigue in the shape-memory alloy after a few stress–strain cycles. In a recent work, researchers crystallographically engineered this alloy's composition (through systematic doping) to precisely satisfy a specific lattice geometry [18,19]. By doing so, they dramatically enhanced the reversible cycling of the shape memory alloy: the resulting alloy not only showed negligible fatigue after ten million cycles but did so despite its large transformation strain and despite being subjected to a load of over 300 MPa. Besides shape-memory alloys, researchers have crystallographically engineered highly reversible microstructures in other phase transformation materials, including ferroelectrics [20–22], fracture-resistant ceramics [23], and semiconductors [24]. These advances in phase transformation materials motivate a new line of research in which the existing intercalation materials can be similarly designed to achieve dramatic enhancement in material lifespan.

In another line of research, the crystallographic texture of intercalation materials can be locally engineered, such as by seeding vacancies or doping grain boundaries, to improve material properties [25]. For example, clusters of vacancy defects have been shown to mediate ion diffusion in intercalation materials [7,26,27]. Similarly, small changes to the local structure and chemistry of a grain boundary (referred to as complexions [28]) can significantly alter battery materials' mechanical and transport properties. Other defects, such as dislocations and antisite defects, which are often viewed as deleterious features, can be tailored to enhance reversible cycling [29]. These examples demonstrate potential opportunities to significantly improve material properties by locally designing the crystallographic texture of intercalation materials.

My central aim is to provide an overview of how crystal symmetry and crystallographic microstructures affect intercalation material properties, and how we can intervene and design these crystallographic features to significantly enhance material behavior. I

Manuscript received March 16, 2022; final manuscript received June 15, 2022; published online August 4, 2022. Assoc. Editor: Partha P. Mukherjee.

address this central theme in three parts. First, I introduce the types of structural transformations of unit cells during intercalation and highlight potential opportunities to design facile structural changes. Second, I review the different phase transformation microstructures that form in intercalation materials and share my perspective on crystallographically designing these microstructural patterns. Finally, I identify various forms of crystal defects and imperfections commonly observed in crystalline solids and discuss the challenges in tailoring these defects to enhance material performance. In this review, I predominantly cite examples from the literature on intercalation cathodes, however, the challenges and potential opportunities I identify are transferable to a broader range of intercalation compounds.

## Structural Transformation

The reversible intercalation of active species into a host-electrode often induces an abrupt structural transformation of its crystal lattices.<sup>1</sup> These structural changes range from displacive transformations (in which atoms undergo cooperative movement resulting in changes to lattice parameters [36]) to transformations accompanied by polyhedral rotations that not only generate significant lattice strains but also affect the electronic structure of the host material [6,12]. These structural transformations impede ion migration, nucleate microcracks, and contribute to the irreversible decay of material properties, see Figs. 1(a)–1(d) [10,30,37,38]. These challenges highlight the need to understand different types of structural transformations and to investigate whether these transformations can be *crystallographically designed* to enhance material properties. In this section, I review the different types of structural transformations primarily using intercalation cathodes as representative examples and identify key challenges and opportunities to design facile transformations.

**Types of Structural Transformation.** A common mode of structural transformation in cathodes is the volumetric dilation of individual lattices on intercalation. For example, inserting lithium into FePO<sub>4</sub> (an olivine compound) increases its *a* and *b* lattice parameters (while simultaneously decreasing the *c* parameter) resulting in a net volume increase of ~6%. This deformation is reversible on lithium extraction, however, can induce microcracking on repeated cycling, see Fig. 1(a). Both the intercalated and reference lattices (e.g., LiFePO<sub>4</sub> and FePO<sub>4</sub>) belong to the same space group and show no reduction in crystal symmetry.<sup>2</sup> Similar symmetry-preserving transformations are observed in commonly used electrodes such as layered LiCoO<sub>2</sub> and Li-NMC [39] and in lithium battery anodes such as Li<sub>4</sub>Ti<sub>5</sub>O<sub>12</sub> [40].

By contrast, cathode compounds such as the manganese spinel, undergo cooperative Jahn–Teller distortion on intercalation and are characterized by an abrupt and spontaneous symmetry breaking of the unit cell [32,41]. For example, electrochemical insertion of lithium into a cubic LiMn<sub>2</sub>O<sub>4</sub> transforms it to a tetragonal Li<sub>2</sub>Mn<sub>2</sub>O<sub>4</sub> unit cell. This cubic-to-tetragonal transformation is often not entirely reversible thus limiting the uptake of active ions [42,43]. However, this symmetry-lowering transformation is necessary for the material to form finely twinned microstructures, see Fig. 1(b). Other transition-metal oxides, such as PNB<sub>9</sub>O<sub>25</sub>, are also accompanied by a tetragonal distortion (from Jahn–Teller effect) of its lattices along the *c*-axis. These structural distortions coupled with the electronic structure of PNB<sub>9</sub>O<sub>25</sub> affect the ordered filling of multiple Li ions [14]. Overall, these abrupt crystallographic changes can induce significant misfit strains between neighboring lattices and collectively generate volume changes. On repeated

intercalation, these structural changes manifest as interfacial stresses leading to microcracking at phase boundaries (see Fig. 1(a)) and delamination at the electrode/electrolyte interfaces [6].

Another mode of structural transformation, which is unique to layered electrodes, is the stacking–sequence–change mechanism [34]. In this type of transformation, intercalation of an active species induces a relative displacement between individual layers of the electrode, however, each layer is topotactically preserved. Figure 1(c) shows a schematic illustration of this stacking–sequence–change mechanism: At first, two layers initially positioned at “A” (i.e., AA layer) transform to an AB configuration on intercalation (i.e., atoms in the lower layer shift to position “B”). Next, on extraction of the intercalant species, the AB configuration transforms to the AA configuration; however, this configuration can be different from its initial AA configuration. That is, the reverse transformation (AB → AA) can result in a relative shift of the two layers. Although these stacking–sequence–change transformations are kinetically unfavorable and rare, they can induce lattice-invariant shearing of electrode particles, leading to characteristic step-formation and microcracking in layered oxides (e.g., Li<sub>x</sub>CoO<sub>2</sub>, Li<sub>x</sub>NiO<sub>2</sub>, Li<sub>x</sub>Ni<sub>y</sub>Mn<sub>z</sub>Co<sub>(1–y–z)</sub>O<sub>2</sub>) [44–46] and sulfides (e.g., Na<sub>x</sub>TiS<sub>2</sub>) [47], see Fig. 1(c). These microstructural changes in layered compounds impact battery performance by contributing to capacity loss and increased polarization with electrochemical cycling [34].

The layered structure of V<sub>2</sub>O<sub>5</sub>, another widely studied intercalation compound, undergoes an unfolding type of structural transformation on deintercalation, see Fig. 1(d) [48,49]. For example, the  $\gamma$ -LiV<sub>2</sub>O<sub>5</sub> structure consists of VO<sub>5</sub> pyramids that share edges and are connected to form ribbons. These ribbons are then connected by pyramid corners that result in a puckered-type of layers with lithium atoms located between the sheets, see Fig. 1(d).<sup>3</sup> On deintercalation, the interlayer separation in  $\gamma$ -LiV<sub>2</sub>O<sub>5</sub> decreases while the interribbon distance increases. This structural transformation is accompanied by an unfolding of the V<sub>2</sub>O<sub>5</sub> layers. On deep discharge of Li<sub>x</sub>V<sub>2</sub>O<sub>5</sub> (i.e., inserting  $x > 2$  Li ions), the cathode becomes increasingly disordered (or amorphous) and contributes to the structural degradation of the material [35,51].

More recently, lithiation-induced polyhedral rotations in perovskite cathodes have been reported as another mode of structural transformation [52]. Perovskite compounds such as ReO<sub>3</sub> have an open framework and can accommodate up to two Li ions. However, recent studies have shown that electrochemical insertion induces a correlated rotation of its polyhedral subunits that not only generate significant lattice strains but also affect the electronic structure of the cathode material. These rotational type of distortions severely impede the reversible capacity of cathodes over extended cycling and demonstrate the need to crystallographically design structural transformations.

These various forms of structural transformations, although they occur at the atomic scale, significantly affect the material’s structural integrity at the continuum scale. For example, intercalation cathodes undergoing crystal–symmetry–lowering transformations collectively generate macroscopic volume changes and internal stresses which, respectively, lead to electrode delamination and fracture. Similarly, the stacking–sequence–change in layered cathodes generates a lattice-invariant shear resulting in microcracking of electrodes. The unfolding transformation of polyhedral ribbons in V<sub>2</sub>O<sub>5</sub> and the polyhedral rotations in perovskite compounds also lead to irreversible structural degradation of intercalation compounds. These structural degradations expose fresh active areas of the electrode to the electrolyte and act as a site for side chemical reactions. These parasitic reactions, in turn, over time contribute to the decay in the electrochemical performance of the intercalation material.

**Designing Structural Transformations.** Researchers have developed different strategies to minimize the deleterious effects

<sup>1</sup>These abrupt changes to the lattice geometry accompanying a first-order phase transformation differ from a gradually changing lattice geometry accompanying a stoichiometric chemical expansion of materials (e.g., Fluorite-Ceria) [36].

<sup>2</sup>Please note that symmetry-preserving structural transformations could still have different lattice geometries.

<sup>3</sup>Further intercalation of lithium leads to the formation of a metastable phase that has been examined as a potential cathode candidate for multivalent ion intercalation [50].

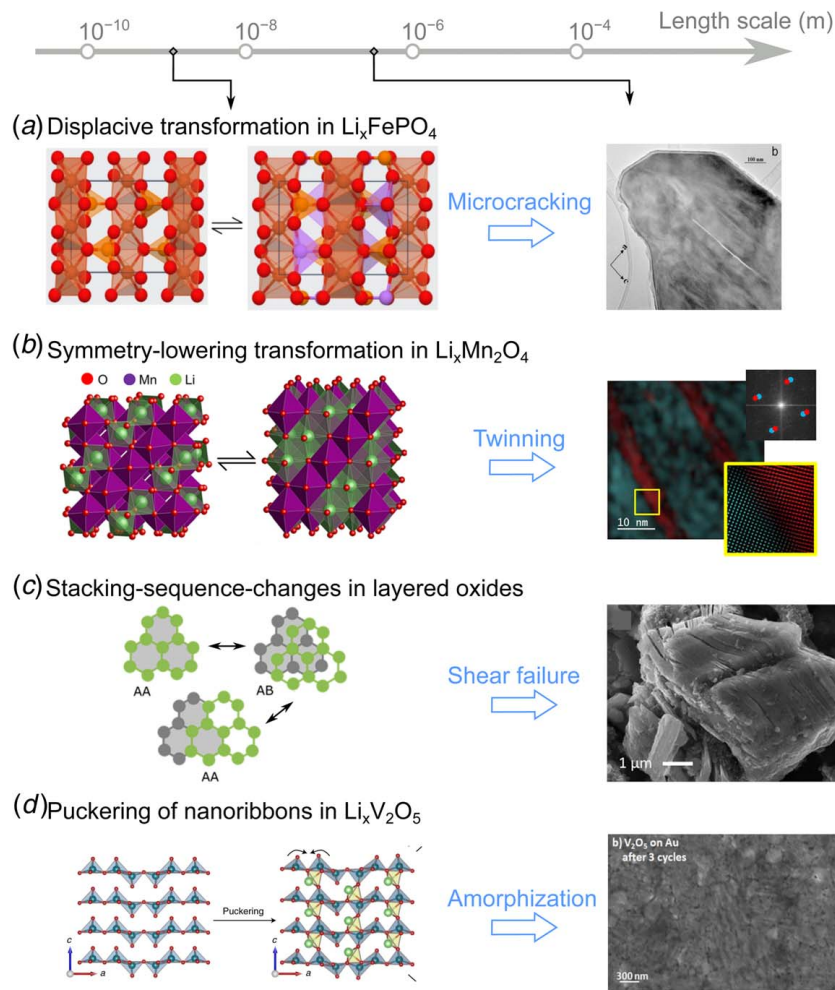


**Fig. 1** Structural transformations of individual lattices generate at the atomic scale ( $\sim 10^{-9}$  m) generate a significant lattice misfit at the continuum scale ( $\sim 100$  nm). These structural transformations manifest in various forms and are directly linked to the structural degradation of intercalation materials as follows. (a) The displacive transformation of individual lattices in  $\text{Li}_x\text{FePO}_4$  induces coherency stresses at the  $\text{FePO}_4/\text{Li}_x\text{FePO}_4$  phase boundary, which in turn nucleates microcracks. Reprinted with permission of IOP Publishing Ltd. from Ref. [30]; © 2013 by [31] under the Creative Commons license CC BY. Published by AIP Publishing. (b) The cubic-to-tetragonal symmetry lowering transformation in  $\text{Li}_x\text{Mn}_2\text{O}_4$  generates a finely twinned mixture that minimizes coherency stresses at the phase boundary. Reprinted with permission from Ref. [32]. © 2020 American Chemical Society. (c) The stacking-sequence-change transformation of lattices in layered oxides contributes to lattice-invariant shear resulting in microcracking of the intercalation compound. Reprinted with permission from Refs. [33,34]. © 2017 American Chemical Society. (d) The polyhedral chains (nanoribbons) in  $\text{Li}_x\text{V}_2\text{O}_5$  unfold and pucker during intercalation resulting in a disordered (or amorphous) phase. Reprinted with permission from Ref. [35]. © 2021 Elsevier.

of structural transformations. In one strategy, called “staging,” researchers diffuse the guest species into select crystallographic channels of the intercalation material (e.g., in graphite systems [53,54]), occupying only a fraction of the intercalation sites and thereby reducing internal stresses in the materials. In other strategies, researchers suppress structural transformations by engineering host materials as nanoparticles, by designing mechanical constraints as epitaxial strains [35] or coherency stresses [55], and by operating intercalation materials within specific voltage windows. While these strategies delay chemo-mechanical degradation of intercalation materials and have improved their lifespans, they do so at the cost of the material’s energy storage capacity and performance [8].

Recent advances in experimental synthesis techniques have opened doors to designing facile structural transformations in intercalation materials. For example, Schofield et al. [56] use a novel

topochemical synthesis route to introduce dopants (e.g., Molybdenum) at selective sites of the cathode  $\text{V}_2\text{O}_5$  compound. By doing so, they not only tailor its lattice parameters with a precision of  $\sim 0.01$  Å but also can accurately design a facile structural transformation mitigating its mechanical degradation with repeated use [56–58]. In another study, Lee et al. [59] identify a zero-strain intercalation cathode  $\text{LiCo}_{1-x}\text{Al}_x\text{O}_2$  ( $0 < x \leq 0.5$ ), which offers negligible volume changes ( $\leq 0.02\%$ ) on intercalation. These techniques have led to the development of novel compounds with reduced structural distortions and are promising candidates to develop zero-strain electrodes [59,60].

These experimental efforts to crystallographically design novel compounds are often complemented by first-principle calculations [61–63]. The first-principle calculations not only provide crucial insights into the structural transformation mechanisms and the chemical stability of

doped compounds but also provide a framework to computationally design novel compounds. For example, a first-principles method was used to systematically study how transition metal substitutions in layered oxide compounds would enhance battery-related properties (e.g., thermodynamic stability, ionic mobility). This computational approach of chemically designing intercalation compounds could be used as a precursor to guide the experimental synthesis of new compounds. Recent developments in high-throughput computing [31,64,65] have led to an enormous database of intercalation materials, for example, The Materials Project, Inorganic Crystal Structure Database, which further guide experimentalists to synthesize new compounds [31,64,66,67]. For example, the carbanophosphates—a new class of cathode materials—were discovered using this high-throughput computational approach [68]. These advances in theoretical and experimental methods provide invaluable tools to design chemical compositions and structural transformations in intercalation materials and accelerate the discovery of novel compounds.

In an ongoing line of research in my group, we develop algorithms to quantify structural transformation pathways in commonly used intercalation materials and establish crystallographic design rules necessary to reduce coherency stresses and volume changes in these materials, see Figs. 2(a) and 2(b). These crystallographic design rules identify precise lattice parameter relationships that an intercalation material must satisfy to have minimum volume changes and coherency stresses during transformation. For example, a self-accommodating microstructure forms in materials with a zero volume change during intercalation. These design rules are described in detail in Ref. [69]. We apply our analytical framework to over 5000 intercalation compounds documented on The Materials Project database to identify candidate compounds that satisfy the crystallographic design rules. These candidate compounds and the crystallographic design rules would guide material chemists to systematically design structural transformation pathways in intercalation compounds. Besides the crystallographic design rules, there is a need to establish chemical substitution charts that identify stable compositions of intercalation compounds on introducing dopants. These charts would assist experimentalists in choosing suitable dopants to alloy intercalation compounds. With the growing need for increased energy densities and the urgency to reuse and recycle materials, it is important to pursue these combined theoretical and experimental approaches to crystallographically design novel compounds.<sup>4</sup>

## Microstructures

The abrupt structural transformation of individual lattices in intercalation electrodes generates significant misfit between neighboring lattices. This lattice misfit manifests at the continuum scale as coherency strains, which in turn nucleate defects and anisotropically expand electrodes, leading to their irreversible damage. Intercalation materials minimize these coherency stresses by forming microstructural patterns. These microstructures can range from a simple two-phase pattern to a complex finely twinned pattern, see Figs. 3(a)–3(c) [32,73]. Besides structural transformations, applied boundary conditions on the electrode and engineering design constraints drive the formation of rich and varied microstructural patterns in intercalation systems, see Figs. 3(d)–3(f) [71,74–77]. How these microstructures nucleate and grow affects rate capabilities and lifespans of intercalation materials [70]. In this section, I review the origin of these phase-separating microstructures in intercalation electrodes and highlight potential opportunities to crystallographically design these microstructures to enhance material longevity and performance.

<sup>4</sup>More recently, researchers are developing novel multivalent intercalation compounds that promise increased energy densities (exchange more than one ion) when compared to the conventional Li-ion batteries. Inserting these multivalent ions into host electrodes, however, is often accompanied by structural degradation because of the typically large ionic radius of the intercalating species. The widespread nature of these chemo-mechanical challenges further emphasizes the need to crystallographically design materials with facile structural transformation pathways.

**Origin of Phase Separation Microstructures.** Phase separating microstructures are characterized by a two-phase coexistence—within a single electrode particle—comprising a Li-rich region (lithiated phase) and a Li-poor region (delithiated phase). These regions are separated by a phase boundary that moves back and forth through the electrode during charge/discharge cycles. Figures 3(a)–3(f) show the types of microstructural patterns that form in intercalation electrodes. In this subsection, I review three key factors that drive the formation of these phase separation microstructures.

First, are the coherency strains that arise from misfit between neighboring lattices. These coherency strains increase the elastic energy of the system and phase separation microstructures form at the continuum scale to minimize these coherency strains, see Figs. 3(a)–3(c). In intercalation electrodes with facile transformations (i.e., minimum crystallographic changes on Li intercalation), such as  $\text{Li}_x\text{FePO}_4$ , the phase boundary has negligible coherency strains and consequently forms phase separating microstructures that resemble the spinodal decomposition patterns, see Fig. 3(a). However, in intercalation electrodes with appreciable coherency strains, such as  $\text{Li}_x\text{Mn}_2\text{O}_4$ , the phase boundaries are elastically stressed. To reduce this elastic stress, the lithiated phase ( $\text{Li}_2\text{Mn}_2\text{O}_4$ ) forms a mixture of finely twinned domains that has an average lattice deformation compatible with the delithiated phase ( $\text{LiMn}_2\text{O}_4$ ), see Fig. 3(b) [32]. These microstructures reduce the coherency stresses at the phase boundary, but at the same time act as a barrier for reversible transformation, leading to irreversible capacity loss of the material [41,43].<sup>5</sup> Finally, in intercalation electrodes with very large lattice misfit (or coherency strains) phase separation is suppressed resulting in a solid-solution type of microstructure [55,79]. In extreme cases, such as  $\text{NaFePO}_4$  the large lattice misfit leads to amorphization of the intercalation compound [11], see Fig. 3(c).

Second, the polycrystalline texture of intercalation electrodes affects the evolution of phase separating microstructures. For example, certain crystallographic orientations facilitate faster diffusion of the intercalating species—this anisotropic diffusion leads to heterogeneous lithiation and charge distribution in the host electrode [80]. Additionally, the random orientation of grains in a polycrystalline electrode creates tortuous diffusion pathways that impede charge/discharge rates. In another example, the heterogeneous lithiation induces inhomogeneous volume changes of the polycrystalline electrode particle. This inhomogeneity generates intergranular stresses that nucleate microcracks and contribute to the irreversible degradation of the electrode [81–83]. Researchers have developed theoretical and experimental tools to crystallographically enhance the performance of polycrystalline electrodes. Recently, Xu et al. [16], demonstrated that architecting the crystallographic orientations of grains in a radial pattern contributes to smaller charge heterogeneity and reduced intergranular stresses in a polycrystalline electrode, see Fig. 5(a). Similarly, researchers have identified grain morphologies and transformation pathways that mitigate structural degradation of electrode particles.

Third, the applied mechanical constraints, such as electrode particle geometry, substrate straining, and curvature-induced stresses, drive the formation of microstructural patterns. The mechanism underlying the formation of these microstructures is complex and is often related to the interplay between electrode geometry and stored elastic energy. For example, the elastic interaction between particle surfaces in a nano-size  $\text{Li}_x\text{FePO}_4$  electrode drive the formation of stripe-like microstructures during intercalation, Fig. 3(d). These microstructures relieve surface energy arising from the nano particle geometry and adopt a periodic stripe-like

<sup>5</sup>These finely twinned microstructures in spinel compounds bear a striking resemblance to the characteristic martensitic microstructures formed by energy minimization in shape-memory alloys [78]. In our recent work, we draw on insights from phase transformation materials such as shape-memory alloys to crystallographically design the phase separation microstructures in intercalation electrodes [69].

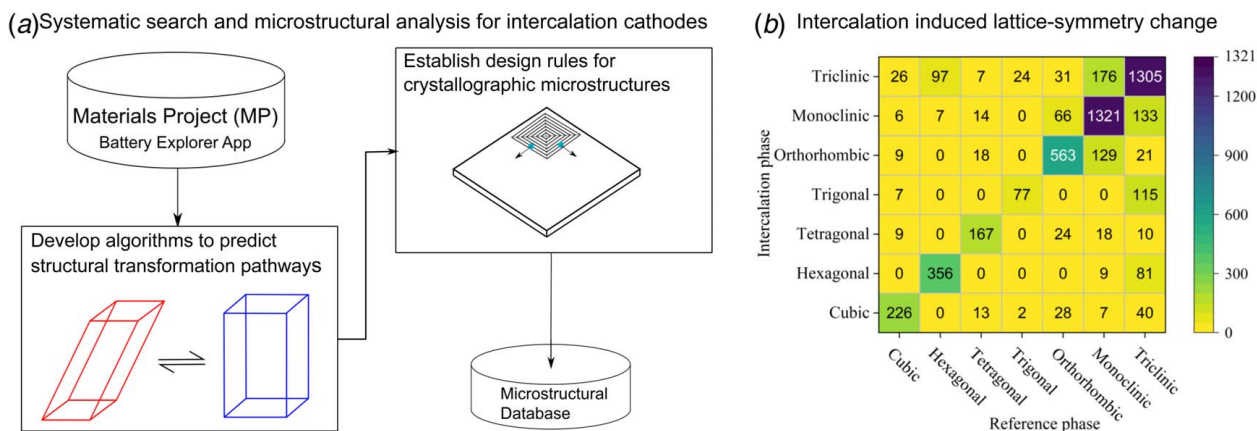


**Fig. 2** (a) We analyze structural transformations in over 5000 intercalation compounds documented on the Materials Project database and identify candidate compounds that satisfy crystallographic design rules to form self-accommodating or highly reversible microstructures. (b) Our analysis shows that only ~10% of known intercalation compounds undergo lattice-symmetry lowering transformations, and thus can form twin boundaries and other crystallographic microstructures. Adapted from Ref. [69].

pattern [55].<sup>6</sup> In another example, the bending deformation of rod-shaped electrodes (in their secondary electrode configuration) stresses the electrode particle and increases the stored elastic energy of the system [71,85]. To minimize this stored energy, phase separation microstructures comprising Li-rich/Li-poor phases form, as shown in Fig. 3(e). These periodic phase separation patterns in the rod-like  $V_2O_5$  electrode reduce the energy penalty arising from the imposed bending constraint. Other mechanical constraints, such as the imposed strains arising from the rigid substrate in a thin-film electrode geometry, have been shown to destabilize the intercalation front [74]. For example, tensile stresses in  $LiFePO_4$  generate a wave-like pattern of the intercalation front, leading to the inhomogeneous lithiation of the electrode, see Fig. 3(f).<sup>7</sup> Overall, the microstructural patterns formed in intercalation electrodes are affected by physical phenomena spanning multiple length scales, ranging from structural transformations of individual lattices at the atomistic scale to concentration inhomogeneities at the continuum scale.

**Designing Microstructural Patterns.** How phase transformation microstructures nucleate and grow in intercalation materials greatly affects their properties. For example, the wave-like microstructural patterns that form under tensile stresses lead to a nonuniform lithiation of the electrode; this nonuniform lithiation can be detrimental contributing to current hotspots and mechanical degradation. Similarly, the phase separating microstructures in  $LiFePO_4$  generate significant coherency stresses during charging/discharging; these coherency stresses can nucleate microcracks, and with repeated intercalation, contribute to material failure. It is important to engineer microstructural patterns to improve material performance and lifespans.

To date, researchers have developed several techniques to design and control microstructural evolution in intercalation materials. For instance, Lim et al. [70] control the electrochemical operating conditions, such as diffusion kinetics, to suppress phase separation microstructures and to instead stabilize a solid solution pattern. This approach minimizes coherency stresses and retains the specific capacity of  $LiFePO_4$ . In another study, Santos et al. [71] impose mechanical constraints, such as engineering epitaxial strains and imposing bending stresses, to modulate the nucleation and growth of phase separation microstructures. This approach demonstrates

how mechanical constraints are an additional design parameter that can be engineered to control the nucleation and growth of microstructural patterns. In addition to designing phase transformation microstructures in intercalation cathodes, researchers engineer electrode particle geometries (e.g., by faceting electrodes along specific crystallographic planes) and the underlying crystallographic texture (e.g., by designing grain orientations) to facilitate rapid charge/discharge capabilities. These approaches to designing microstructural patterns in intercalation electrodes have improved its electrochemical performance and extended its lifespans.

In addition to these ongoing efforts, I propose a new line of research in which we *crystallographically design* microstructures in intercalation materials to achieve a dramatic improvement of material properties. Although phase transformation microstructures evolve at the continuum length scale, their origin is closely related to how individual lattices deform at the atomic scale. This exact correspondence between continuum microstructures and atomic lattice deformations is formalized via a Cauchy–Born rule that forms the basis for this proposed line of research [86].<sup>8</sup> This rule has been successfully applied to crystallographically design microstructures in other phase transformation materials—such as shape-memory alloys, ferromagnets, and ferroelectrics—which bear striking similarities to intercalation compounds (e.g., finely twinned microstructures).

For example, Chluba and co-workers systematically dope a  $Ti_{51}Ni_{36}Cu_{13}$  shape-memory alloy to satisfy a specific combination of lattice parameters for which a stress-free phase boundary forms [18]. This alloy typically develops fatigue after 200 stress–strain cycles, however by crystallographically designing its microstructure (via doping), researchers discovered a novel alloy composition  $Ti_{54}Ni_{34}Cu_{12}$  that shows negligible fatigue despite cycling it for ten million times. Similarly, crystallographic designing of microstructures has been used to engineer self-accommodating patterns (which accommodate with the macroscopic material shape and have zero volume changes) and twin interfaces, and this strategy has been applied to materials beyond shape-memory alloys [20,23,24]. These results highlight potential opportunities for crystallographic designing of microstructures in intercalation materials.<sup>9</sup>

These advances in the crystallographic designing of materials would need to be complemented by developments in theoretical and experimental frameworks. For example, it is important to understand how the crystallographic texture of the intercalation material

<sup>6</sup>By contrast in relatively large electrodes, e.g., micro-sized  $Li_1FePO_4$ , the bulk elastic energy plays a dominant role, leading to mosaic-like patterns during intercalation, see Fig. 3(a) [84].

<sup>7</sup>In another line of research, mechanical constraints, such as substrate strains, have been used to delay the onset of large structural transformations in thin film electrodes [35].

<sup>8</sup>The Cauchy–Born rule is used together with the energy minimization theory to explain the origin of microstructures and more recently to design microstructural patterns that are stress-free and are highly reversible.

<sup>9</sup>Here, crystallographic designing refers to systematic doping of intercalation compounds to tailor lattice geometries and stabilize shape-memory-like microstructures.

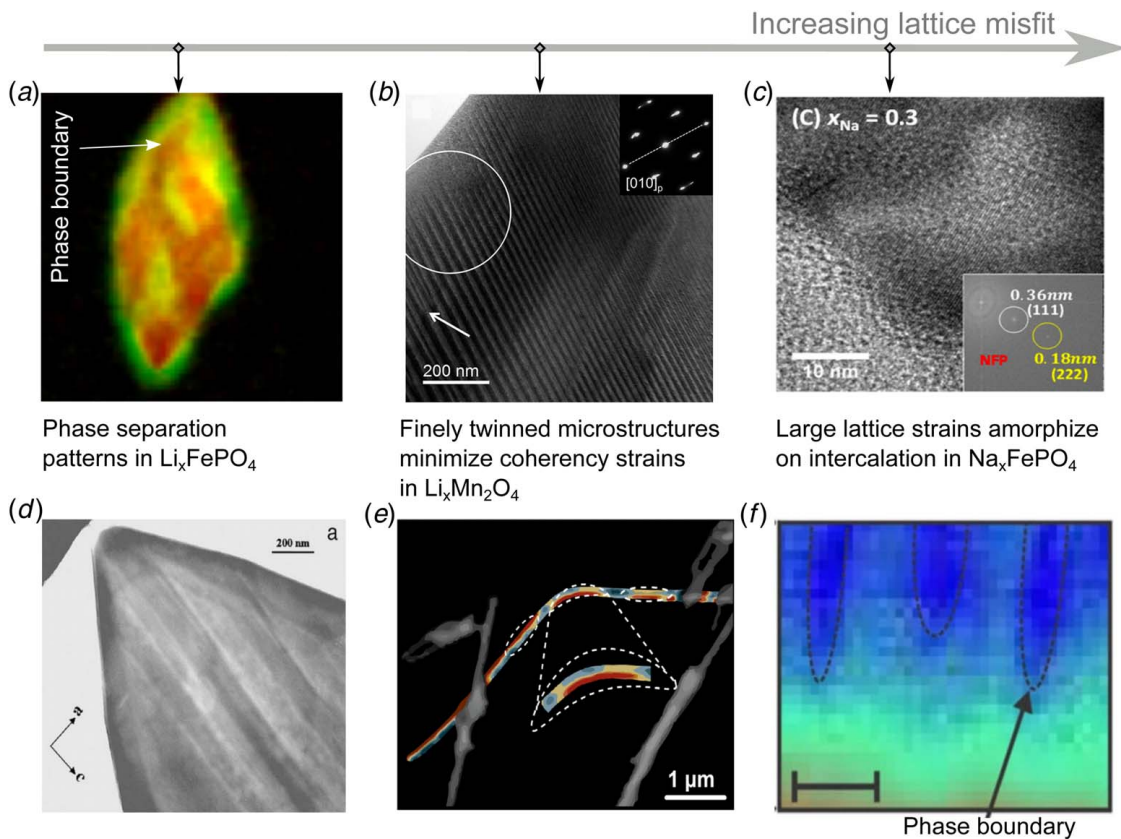


**Fig. 3** Phase separation microstructures form to reduce the chemo-mechanical energy of the system. Intrinsic lattice misfit generates a wide range of microstructures: (a) For small lattice misfit spinodal decomposition patterns (such as in  $\text{Li}_x\text{FePO}_4$ ) form during intercalation. Reprinted with permission from Ref. [70]. © 2016 AAAS. (b) Other microstructures such as finely twinned martensite-like mixtures form in  $\text{Li}_x\text{Mn}_2\text{O}_4$  to reduce the coherency stresses between lithiated and delithiated phases. Reprinted with permission from Ref. [32]. © 2020 American Chemical Society. (c) For extremely large lattice misfit (>20%) a disordered phase such as in  $\text{Na}_x\text{FePO}_4$  forms during intercalation. Reprinted with permission from Ref. [11]. © 2017 American Chemical Society. Other external constraints drive microstructural patterns: (d) electrode particle size (and surface energy effects) generates a stripe-like microstructural pattern in  $\text{Li}_{0.5}\text{FePO}_4$ ; Reprinted with permission of IOP Publishing Ltd. from Ref. [30]. © 2006 The Electrochemical Society. (e) Bending deformation stresses drives phase separation patterns in  $\text{Li}_x\text{V}_2\text{O}_5$ ; © 2020 by [71] under the Creative Commons license CC BY-NC. Published by Royal Society of Chemistry. (f) Epitaxial strains generate a wave-like pattern of the intercalation front in  $\text{Li}_x\text{FePO}_4$ . Reprinted with permission from Ref. [72]. © 2015 Springer Nature.

interacts with the diffusing species during intercalation. At present, material models typically describe microstructures in intercalation materials as a function of a continuum field variable (e.g., Li-composition) [87]. These models provide important insights into the structure of a phase boundary [88], interfacial dynamics [89], and stress evolution [90] in intercalation materials. These models, however, do not account for the underlying heterogeneous lattice deformations in a polycrystalline material. To address this gap, we will need a rigorous mathematical framework that couples the interaction between the crystallographic texture of the intercalation material and the Li-composition diffusion. Previously developed phase-field frameworks for chemo-mechanical materials, such as combining the Cahn–Hilliard model with a phase-field-crystal model, would be an initial step in this direction [91,92]. These mathematical models would reveal crucial insights into the origin of crystallographic microstructures and assist experimentalists to probe microstructural evolution in intercalation compounds.

## Defects

Crystallographic defects are interruptions to the regular periodic crystal lattice and are widely observed in intercalation electrodes. These defects form during synthesis, processing, or electrochemical cycling of intercalation materials and have been shown to have a significant impact on its mechanical and transport properties. On the one

hand, dislocation defects that nucleate during electrochemical cycling perturb the sequential arrangement of crystallographic planes and contribute to the electrode's irreversible voltage fade [94]. On the other hand, crystallographic defects such as clusters of vacancies can enhance electrode conductivity by mediating Li diffusion in intercalation electrodes [7]. In this section, we consider three families of crystallographic defects—namely point, line, and planar defects—and review how they affect an intercalation compound's chemo-mechanical properties, see Fig. 4. We conclude this section by identifying challenges and opportunities in engineering defects in intercalation materials and improving material properties.

**Types of Crystallographic Defects.** Point defects are zero-dimensional atomic imperfections that occur only at a single lattice point and common examples include vacancies, dopants, and antisite defects. These defects, although considered as deleterious features, can have conducive effects on ionic mobility, lattice structural transformations, and phase transformation kinetics. For example, the antisite defects in  $\text{LiFePO}_4$  block Li movement along the [010] migration channel, however simultaneously increase Li mobility along other crystallographic directions, contributing to an order-of-magnitude improvement in phase transformation kinetics [29]. Another example is the trace doping of a cation (Ti) into an intercalation compound (e.g.,  $\text{LiCoO}_2$ ). These dopants segregate at particle surfaces and/or at grain boundaries and induce microstrains in the electrode,

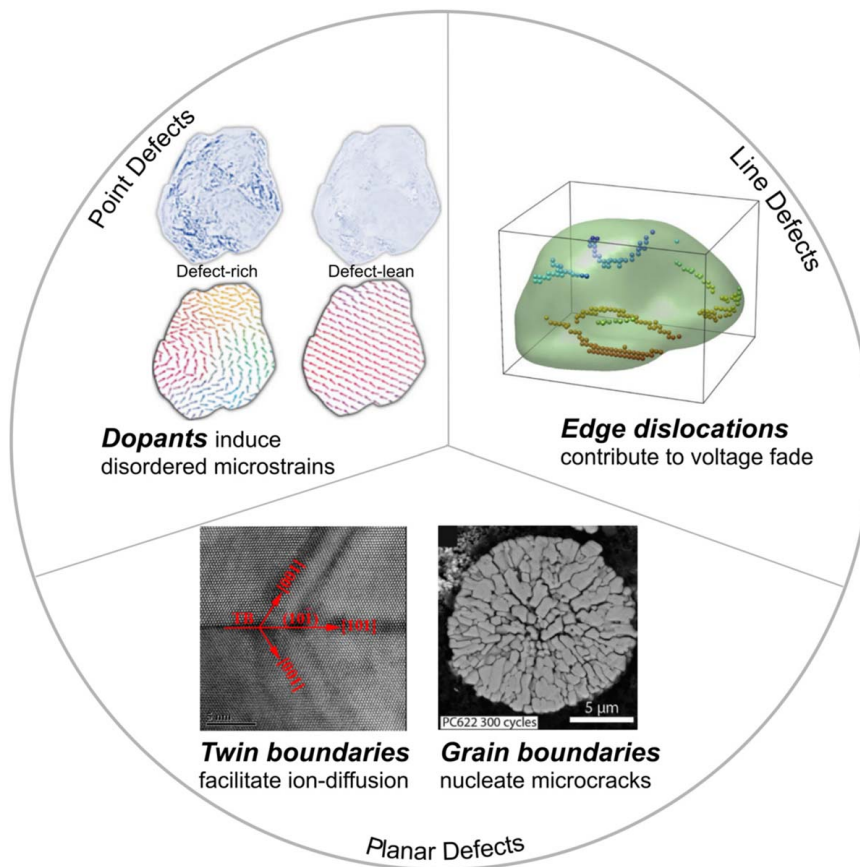


**Fig. 4** Commonly observed crystal defects in intercalation compounds can be categorized into (Clockwise) point defects (e.g., dopants, vacancies), line defects (e.g., edge-dislocations), and planar defects (e.g., twin boundaries, grain boundaries). These crystal defects can form either during manufacturing or during electrochemical cycling and can adversely affect the performance of the battery. Reprinted by permissions from Refs. [93,96]. © 2020 Elsevier. Reprinted with permission from Ref. [94]. © 2018 Springer Nature. Reprinted with permission from Ref. [95]. © 2015 American Chemical Society.

see Fig. 4. These internal strains suppress phase separation and facilitate longer lifespans of layered compounds [93].

Line defects are one-dimensional imperfections that correspond to a misaligned arrangement of atoms. A widely observed line defect is an edge-dislocation defect that corresponds to an abruptly terminated plane of atoms in the material bulk. These dislocation defects nucleate during electrochemical cycling and are found to be mobile [17,94]. For example, in layered oxide electrodes, the nucleation and migration of dislocations disrupt the stacking sequence of layers in the host electrode. These structural changes are shown to block Li migration pathways and contribute to the voltage fade of the cathode particle [94]. In other electrodes, such as the spinel compounds, dislocations nucleate in the vicinity of a phase boundary to relieve coherency stresses. Although dislocation defects mitigate coherency stresses via plastic deformation, excessive accumulation of dislocations contributes to the irreversible transformation of the electrode [32,97].

Planar defects are two-dimensional and typically correspond to interfacial regions separating domains with differing crystallographic orientation. Common examples of planar defects include grain boundaries, twin boundaries, and stacking faults. These defects can have both positive and negative impacts on material properties. On the one hand, planar defects such as twin boundaries are shown to have a lower barrier for ionic diffusion and thus facilitate faster lithium transport. Engineering these planar defects in intercalation cathodes, such as spinel compounds, has led to its fast-charging properties [95,98]. On the other hand, planar defects such as grain boundaries are shown to be sites of microcracking and fracture in

polycrystalline electrodes. For example, the anisotropic volume changes of individual grains during intercalation generates interfacial stresses at the grain boundary, which at critical values leads to inter granular fracture [99]. These fractured interfaces lead to the loss of ionic contact and contribute to the local impedance in cathodes.

Crystal defects—point, line, or planar—commonly occur in intercalation materials and/or nucleate on repeated intercalation. These defects interact with Li-diffusion front during charging/discharging processes and can adversely impact a material’s mechanical and transport properties.

**Designing Crystallographic Defects.** In this subsection, I argue that although crystal defects are deleterious features of intercalation materials impeding electrochemical performance, select crystal defects can be crystallographically engineered to enhance the material’s mechanical and transport properties. I present case studies in which researchers have engineered defects—antisite defects (point defect) and grain boundaries (planar defects)—to improve intercalation electrode performance. I will conclude this subsection by identifying open questions and opportunities to systematically design crystal defects in intercalation materials.

Antisite defects are point defects that are generated when a cation (that is typically less mobile) occupies the site of an intercalating ion. These antisite defects block the ion-diffusion pathways in intercalation materials and can negatively impact its transport properties [100]. One approach is to remove these antisite defects by structural annealing of electrodes and to open the ion-diffusion pathways

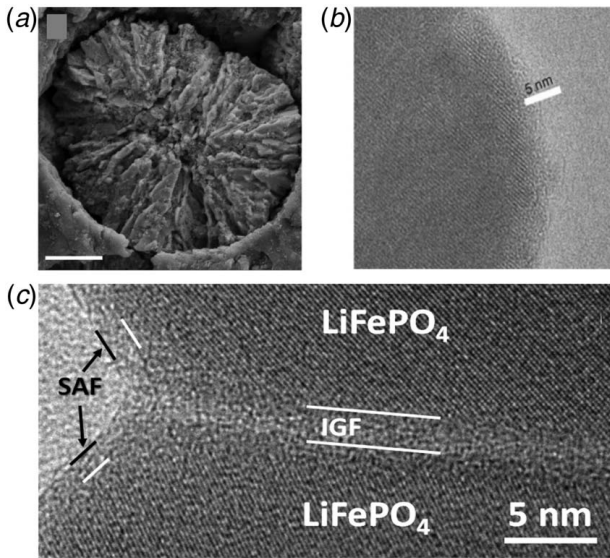


**Fig. 5** Select crystal defects can be engineered into intercalation compounds to improve its properties. (a) By designing a polycrystalline Ni-Mn-Co intercalation cathode with radially oriented grains Xu et al. [16] create less tortuous ion-diffusion pathways. © 2020 by [16] under the Creative Commons license CC BY. Published by Springer Nature. (b) An amorphous surficial layer on LiFePO<sub>4</sub> compound facilitates faster adsorption and ion-exchange rate between electrode and electrolyte [102]. Reprinted with permission from Ref. [102]. © 2009 Springer Nature. (c) Kayyar et al. [103] stabilize amorphous films along grain boundaries which facilitate faster ion-diffusion in intercalation compounds. Reprinted with permission from Ref. [103]. © 2009 AIP Publishing.

[101]. By contrast, another approach is to engineer antisite defects to enhance ion movement along other diffusion pathways and therefore contribute to a collective improvement of material's rate capability. Tang and co-workers use a phase-field framework to show how intercalation materials with anisotropic diffusion (i.e., ion migrates predominantly along 1D channels) can be engineered with antisite defects to enhance ion diffusivity along two-dimensions [29]. This improvement accelerates phase transformation rates by an order of magnitude and facilitates uniform surface reactions in electrode particles.

Grain boundary defects are ubiquitous in intercalation materials and, as discussed above, serve as sites for microcracking and fracture. While these chemo-mechanical challenges can be overcome by synthesizing high-quality single crystal particles, these synthesis methods often require high-temperature and pristine environments. Alternatively, planar defects, such as grain boundaries and surficial films, can be thermodynamically engineered to achieve a dramatic improvement in cohesive and conductive properties, see Figs. 5(b) and 5(c). For example, Kang and Ceder stabilize a fast ion-conducting surface phase on LiFePO<sub>4</sub> particles, which increases its power rate by two orders of magnitude [102]. The disordered nature of the coating material on LiFePO<sub>4</sub> facilitates increased Li<sup>+</sup> adsorption from the electrolyte. Similar disordered films have been stabilized by Luo and co-workers both on electrode particle surfaces and at their grain boundaries to greatly enhance charging/discharging capabilities. These surface films and intergranular films are abrupt transformations of crystalline interfaces and can be systematically designed (e.g., controlled processing conditions, introducing dopants, architecting grain boundary morphologies) to optimize battery material properties [103].<sup>10</sup>

<sup>10</sup>In another line of research grain boundary complexions are being applied to anode electrodes to suppress the formation of solid-electrolyte interphase [25].

These case studies demonstrate how small changes to the structure and composition of electrodes can dramatically improve their properties, however, it is unclear on how to experimentally design and optimize these crystal defects. For example, antisite defects accelerate phase transformation rates in electrode particles, however, we do not know what concentration of antisite defects and/or electrode particle geometries that would enhance electrode properties. Similarly, grain boundary complexions dramatically alter a material's cohesive and transport properties, however, the precise thermodynamic-and-kinetic conditions and grain boundary morphologies for which these complexions can be stabilized are not well understood. These examples highlight a need to establish design charts, such as complexion phase diagrams and defect density charts, to systematically engineer crystal defects in intercalation materials [104]. For example, Luo and co-workers use advanced experimental methods, such as X-ray photo-electron spectroscopy and high-resolution transmission electron microscopy (TEM), to characterize interfacial complexions [105]. These experimental techniques provide insights into the mechanism of grain boundary transformation and the stability of complexions in electrochemical environments. Furthermore, advances in large-scale physics-based simulations and data-driven methods are promising tools to elucidate the delicate interplay between grain boundary morphologies, thermodynamic variables, and kinetic conditions [106]. These studies contribute to establishing complexion phase diagrams, which would serve as design charts and guide crystal chemists to systematically engineer interfacial defects in intercalation materials [107].

## Summary

In summary, intercalation materials hold great promise for reversible energy storage but are plagued by chemo-mechanical challenges that limit their performance and lifespans. In this review, I outlined these challenges stemming from structural transformations of individual lattices, collective evolution of phase transformation microstructures, and nucleation and growth of crystal defects. To mitigate these challenges, I identified potential opportunities of how we can intervene and crystallographically design intercalation compounds to enhance their properties and lifespans. I hope that these opportunities can inspire new solutions to the crystallographic designing of intercalation materials.

## Conflict of Interest

There are no conflicts of interest.

## Data Availability Statement

The authors attest that all data for this study are included in the paper.

## References

- [1] Sood, A., Poletayev, A. D., Cogswell, D. A., Csernica, P. M., Mefford, J. T., Fraggedakis, D., Toney, M. F., Lindenberg, A. M., Bazant, M. Z., and Chueh, W. C., 2021, "Electrochemical Ion Insertion From the Atomic to the Device Scale," *Nat. Rev. Mater.*, **6**(9), pp. 847–867.
- [2] Padhi, A. K., Nanjundaswamy, K. S., and Goodenough, J. B., 1997, "Phospho-olivines As Positive-Electrode Materials for Rechargeable Lithium Batteries," *J. Electrochem. Soc.*, **144**(4), p. 1188.
- [3] Chen, S., Wang, Z., Ren, H., Chen, Y., Yan, W., Wang, C., Li, B., Jiang, J., and Zou, C., 2019, "Gate-Controlled VO<sub>2</sub> Phase Transition for High-Performance Smart Windows," *Sci. Adv.*, **5**(3), p. eaav6815.
- [4] Liu, X.-C., Zhao, S., Sun, X., Deng, L., Zou, X., Hu, Y., Wang, Y.-X., Chu, C.-W., Li, J., Wu, J. et al., 2020, "Spontaneous Self-Intercalation of Copper Atoms Into Transition Metal Dichalcogenides," *Sci. Adv.*, **6**(7), p. eaay4092.
- [5] Pothanamkandathil, V., Fortunato, J., and Gorski, C. A., 2020, "Electrochemical Desalination Using Intercalating Electrode Materials: A Comparison of Energy Demands," *Environ. Sci. Technol.*, **54**(6), pp. 3653–3662.

- [6] Lewis, J. A., Tippens, J., Cortes, F. J. Q., and McDowell, M. T., 2019, "Chemo-Mechanical Challenges in Solid-State Batteries," *Trends Chem.*, **1**(9), pp. 845–857.
- [7] Van der Ven, A., Bhattacharya, J., and Belak, A. A., 2013, "Understanding Li Diffusion in Li-Intercalation Compounds," *Acc. Chem. Res.*, **46**(5), pp. 1216–1225.
- [8] Radin, M. D., Hy, S., Sina, M., Fang, C., Liu, H., Vinckeviciute, J., Zhang, M., Whittingham, M. S., Meng, Y. S., and Van der Ven, A., 2017, "Narrowing the Gap Between Theoretical and Practical Capacities in Li-Ion Layered Oxide Cathode Materials," *Adv. Energy Mater.*, **7**(20), p. 1602888.
- [9] Rong, Z., Malik, R., Canepa, P., Gautam, G. S., Liu, M., Jain, A., Persson, K., and Ceder, G., 2015, "Materials Design Rules for Multivalent Ion Mobility in Intercalation Structures," *Chem. Mater.*, **27**(17), pp. 6016–6021.
- [10] Koerver, R., Aygün, I., Leichtweiß, T., Dietrich, C., Zhang, W., Binder, J. O., Hartmann, P., Zeier, W. G., and Janek, J., 2017, "Capacity Fade in Solid-State Batteries: Interphase Formation and Chemomechanical Processes in Nickel-Rich Layered Oxide Cathodes and Lithium Thiophosphate Solid Electrolytes," *Chem. Mater.*, **29**(13), pp. 5574–5582.
- [11] Xiang, K., Xing, W., Ravnsbæk, D. B., Hong, L., Tang, M., Li, Z., Wiaderek, K. M., Borkiewicz, O. J., Chapman, K. W., Chupas, P. J., et al., 2017, "Accommodating High Transformation Strains in Battery Electrodes Via the Formation of Nanoscale Intermediate Phases: Operando Investigation of Olivine NaFePO<sub>4</sub>," *Nano Lett.*, **17**(3), pp. 1696–1702.
- [12] Bucci, G., Talamini, B., Balakrishna, A. R., Chiang, Y.-M., and Carter, W. C., 2018, "Mechanical Instability of Electrode-Electrolyte Interfaces in Solid-State Batteries," *Phys. Rev. Mater.*, **2**(10), p. 105407.
- [13] Christensen, C. K., Mamakhel, M. A. H., Balakrishna, A. R., Iversen, B. B., Chiang, Y.-M., and Ravnsbæk, D. B., 2019, "Order–Disorder Transition in Nano-Rutile TiO<sub>2</sub> Anodes: A High Capacity Low-Volume Change Li-Ion Battery Material," *Nanoscale*, **11**(25), pp. 12347–12357.
- [14] Saber, M., Preefer, M. B., Kolli, S. K., Zhang, W., Laurita, G., Dunn, B., Seshadri, R., and Van der Ven, A., 2021, "Role of Electronic Structure in Li Ordering and Chemical Strain in the Fast Charging Wadsley–Roth Phase P<sub>2</sub>Nb<sub>9</sub>O<sub>25</sub>," *Chem. Mater.*, **33**(19), pp. 7755–7766.
- [15] Balke, N., Jesse, S., Morozovska, A. N., Eliseev, E., Chung, D. W., Kim, Y., Adamczyk, L., Garcia, R. E., Dudney, N., and Kalinin, S. V., 2010, "Nanoscale Mapping of Ion Diffusion in a Lithium-Ion Battery Cathode," *Nat. Nanotechnol.*, **5**(10), pp. 749–754.
- [16] Xu, Z., Jiang, Z., Kuai, C., Xu, R., Qin, C., Zhang, Y., Rahman, M. M., Wei, C., Nordlund, D., Sun, C.-J., et al., 2020, "Charge Distribution Guided by Grain Crystallographic Orientations in Polycrystalline Battery Materials," *Nat. Commun.*, **11**(1), pp. 1–9.
- [17] Ulvestad, A., Singer, A., Clark, J. N., Cho, H. M., Kim, J. W., Harder, R., Maser, J., Meng, Y. S., and Shpyrko, O. G., 2015, "Topological Defect Dynamics in Operando Battery Nanoparticles," *Science*, **348**(6241), pp. 1344–1347.
- [18] Chluba, C., Ge, W., de Miranda, R. L., Strobel, J., Kienle, L., Quandt, E., and Wuttig, M., 2015, "Ultralow-Fatigue Shape Memory Alloy Films," *Science*, **348**(6238), pp. 1004–1007.
- [19] Song, Y., Chen, X., Dabade, V., Shield, T. W., and James, R. D., 2013, "Enhanced Reversibility and Unusual Microstructure of a Phase-Transforming Material," *Nature*, **502**(7469), pp. 85–88.
- [20] Wegner, M., Gu, H., James, R. D., and Quandt, E., 2020, "Correlation Between Phase Compatibility and Efficient Energy Conversion in Zr-Doped Barium Titanate," *Sci. Rep.*, **10**(1), pp. 1–8.
- [21] Muench, I., Balakrishna, A. R., and Huber, J. E., 2019, "Periodic Boundary Conditions for the Simulation of 3D Domain Patterns in Tetragonal Ferroelectric Material," *Arch. Appl. Mech.*, **89**(6), pp. 955–972.
- [22] Balakrishna, A. R., Huber, J. E., and Muench, I., 2016, "Nanoscale Periodic Domain Patterns in Tetragonal Ferroelectrics: A Phase-Field Study," *Phys. Rev. B*, **93**(17), p. 174120.
- [23] Pang, E. L., McCandler, C. A., and Schuh, C. A., 2019, "Reduced Cracking in Polycrystalline ZrO<sub>2</sub>–CeO<sub>2</sub> Shape-Memory Ceramics by Meeting the Cofactor Conditions," *Acta Mater.*, **177**, pp. 230–239.
- [24] Liang, Y. G., Lee, S., Yu, H. S., Zhang, H. R., Liang, Y. J., Zavalij, P. Y., Chen, X., James, R. D., Bendersky, L. A., Davydov, A. V., et al., 2020, "Tuning the Hysteresis of a Metal–Insulator Transition Via Lattice Compatibility," *Nat. Commun.*, **11**(1), pp. 1–8.
- [25] Yan, Q., Whang, G., Wei, Z., Ko, S.-T., Sautet, P., Tolbert, S. H., Dunn, B. S., and Luo, J., 2020, "A Perspective on Interfacial Engineering of Lithium Metal Anodes and Beyond," *Appl. Phys. Lett.*, **117**(8), p. 080504.
- [26] Van der Ven, A., Yu, H.-C., Ceder, G., and Thornton, K., 2010, "Vacancy Mediated Substitutional Diffusion in Binary Crystalline Solids," *Prog. Mater. Sci.*, **55**(2), pp. 61–105.
- [27] Islam, M. S., and Fisher, C. A. J., 2014, "Lithium and Sodium Battery Cathode Materials: Computational Insights Into Voltage, Diffusion and Nanostructural Properties," *Chem. Soc. Rev.*, **43**(1), pp. 185–204.
- [28] Cantwell, P. R., Tang, M., Dillon, S. J., Luo, J., Rohrer, G. S., and Harmer, M. P., 2014, "Grain Boundary Complexions," *Acta Mater.*, **62**, pp. 1–48.
- [29] Hong, L., Yang, K., and Tang, M., 2019, "A Mechanism of Defect-Enhanced Phase Transformation Kinetics in Lithium Iron Phosphate Olivine," *npj Comput. Mater.*, **5**(1), pp. 1–9.
- [30] Chen, G., Song, X., and Richardson, T. J., 2006, "Electron Microscopy Study of the LiFePO<sub>4</sub> to FePO<sub>4</sub> Phase Transition," *Electrochem. Solid-State Lett.*, **9**(6), p. A295.
- [31] Jain, A., Ong, S. P., Hautier, G., Chen, W., Richards, W. D., Dacek, S., Cholia, S., Gunter, D., Skinner, D., Ceder, G., et al., 2013, "Commentary: The Materials Project: A Materials Genome Approach to Accelerating Materials Innovation," *APL Mater.*, **1**(1), p. 011002.
- [32] Erichsen, T., Pfeiffer, B., Roddatis, V., and Volkert, C. A., 2020, "Tracking the Diffusion-Controlled Lithiation Reaction of LiMn<sub>2</sub>O<sub>4</sub> by In Situ TEM," *ACS Appl. Energy Mater.*, **3**(6), pp. 5405–5414.
- [33] Alvarado, J., Ma, C., Wang, S., Nguyen, K., Kodur, M., and Meng, Y. S., 2017, "Improvement of the Cathode Electrolyte Interphase on P2-Na<sub>2/3</sub>Ni<sub>1/3</sub>Mn<sub>2/3</sub>O<sub>2</sub> by Atomic Layer Deposition," *ACS Appl. Mater. Interfaces*, **9**(31), pp. 26518–26530.
- [34] Radin, M. D., Alvarado, J., Meng, Y. S., and Van der Ven, A., 2017, "Role of Crystal Symmetry in the Reversibility of Stacking–Sequence Changes in Layered Intercalation Electrodes," *Nano Lett.*, **17**(12), pp. 7789–7795.
- [35] Zhang, D., Sheth, J., Sheldon, B. W., and Balakrishna, A. R., 2021, "Film Strains Enhance the Reversible Cycling of Intercalation Electrodes," *J. Mech. Phys. Solids*, **155**, p. 104551.
- [36] Bishop, S. R., Marrocchelli, D., Chatzichristodoulou, C., Perry, N. H., Mogensen, M. B., Tuller, H. L., and Wachsman, E. D., 2014, "Chemical Expansion: Implications for Electrochemical Energy Storage and Conversion Devices," *Annu. Rev. Mater. Res.*, **44**, pp. 205–239.
- [37] Kim, K., and Siegel, D. J., 2019, "Correlating Lattice Distortions, Ion Migration Barriers, and Stability in Solid Electrolytes," *J. Mater. Chem. A*, **7**(7), pp. 3216–3227.
- [38] Tealdi, C., Heath, J., and Islam, M. S., 2016, "Feeling the Strain: Enhancing Ionic Transport in Olivine Phosphate Cathodes for Li- and Na-Ion Batteries Through Strain Effects," *J. Mater. Chem. A*, **4**(18), pp. 6998–7004.
- [39] Whittingham, M. S., 2004, "Lithium Batteries and Cathode Materials," *Chem. Rev.*, **104**(10), pp. 4271–4302.
- [40] Verde, M. G., Baggetto, L., Balke, N., Veith, G. M., Seo, J. K., Wang, Z., and Meng, Y. S., 2016, "Elucidating the Phase Transformation of Li<sub>4</sub>Ti<sub>5</sub>O<sub>12</sub> Lithiation at the Nanoscale," *ACS Nano*, **10**(4), pp. 4312–4321.
- [41] Rossouw, M. H., De Kock, A., De Picciotto, L. A., Thackeray, M. M., David, W. I. F., and Ibberson, R. M., 1990, "Structural Aspects of Lithium–Manganese–Oxide Electrodes for Rechargeable Lithium Batteries," *Mater. Res. Bull.*, **25**(2), pp. 173–182.
- [42] Huang, H., Vincent, C. A., and Bruce, P. G., 1999, "Correlating Capacity Loss of Stoichiometric and Nonstoichiometric Lithium Manganese Oxide Spinel Electrodes With Their Structural Integrity," *J. Electrochem. Soc.*, **146**(10), p. 3649.
- [43] Thackeray, M. M., Croy, J. R., Lee, E., Gutierrez, A., He, M., Park, J. S., Yonemoto, B. T., Long, B. R., Blauwkamp, J. D., Johnson, C. S., et al., 2018, "The Quest for Manganese-Rich Electrodes for Lithium Batteries: Strategic Design and Electrochemical Behavior," *Sustain. Energy Fuels*, **2**(7), pp. 1375–1397.
- [44] Amatucci, G. G., Tarascon, J. M., and Klein, L. C., 1996, "CoO<sub>2</sub>, The End Member of the Li<sub>x</sub>CoO<sub>2</sub> Solid Solution," *J. Electrochem. Soc.*, **143**(3), p. 1114.
- [45] Van der Ven, A., Aydinol, M. K., Ceder, G., Kresse, G., and Hafner, J., 1998, "First-Principles Investigation of Phase Stability in Li<sub>x</sub>CoO<sub>2</sub>," *Phys. Rev. B*, **58**(6), p. 2975.
- [46] Croguennec, L., Poullier, C., Mansour, A. N., and Delmas, C., 2001, "Structural Characterisation of the Highly Deintercalated Li<sub>x</sub>Ni<sub>1-x</sub>O<sub>2</sub> Phases (With  $x \leq 0.30$ ) Basis of a Presentation Given at Materials Discussion No. 3, 26–29 September, 2000, University of Cambridge, UK," *J. Mater. Chem.*, **11**(1), pp. 131–141.
- [47] Vinckeviciute, J., Radin, M. D., and Van der Ven, A., 2016, "Stacking–Sequence Changes and Na Ordering in Layered Intercalation Materials," *Chem. Mater.*, **28**(23), pp. 8640–8650.
- [48] Cocciantelli, J. M., Gravereau, P., Doumerc, J. P., Pouchard, M., and Hagemuller, P., 1991, "On the Preparation and Characterization of a New Polymorph of V<sub>2</sub>O<sub>5</sub>," *J. Solid State Chem.*, **93**(2), pp. 497–502.
- [49] Cocciantelli, J. M., Menetrier, M., Delmas, C., Doumerc, J. P., Pouchard, M., and Hagemuller, P., 1992, "Electrochemical and Structural Characterization of Lithium Intercalation and Deintercalation in the  $\gamma$ -LiV<sub>2</sub>O<sub>5</sub> Bronze," *Solid State Ionics*, **50**(1–2), pp. 99–105.
- [50] Andrews, J. L., Mukherjee, A., Yoo, H. D., Parija, A., Marley, P. M., Fakra, S., Prendergast, D., Cabana, J., Klie, R. F., and Banerjee, S., 2018, "Reversible Mg-Ion Insertion in a Metastable One-Dimensional Polymorph of V<sub>2</sub>O<sub>5</sub>," *Chem*, **4**(3), pp. 564–585.
- [51] Christensen, C. K., Sørensen, D. R., Hvam, J., and Ravnsbæk, D. B., 2018, "Structural Evolution of Disordered Li<sub>x</sub>V<sub>2</sub>O<sub>5</sub> Bronzes in V<sub>2</sub>O<sub>5</sub> Cathodes for Li-Ion Batteries," *Chem. Mater.*, **31**(2), pp. 512–520.
- [52] Bashian, N. H., Zhou, S., Zuba, M., Ganose, A. M., Stiles, J. W., Ee, A., Ashby, D. S., Scanlon, D. O., Piper, L. F. J., Dunn, B., et al., 2018, "Correlated Polyhedral Rotations in the Absence of Polarons During Electrochemical Insertion of Lithium in ReO<sub>3</sub>," *ACS Energy Lett.*, **3**(10), pp. 2513–2519.
- [53] Dahn, J. R., Dahn, D. C., and Haering, R. R., 1982, "Elastic Energy and Staging in Intercalation Compounds," *Solid State Commun.*, **42**(3), pp. 179–183.
- [54] Xu, J., Dou, Y., Wei, Z., Ma, J., Deng, Y., Li, Y., Liu, H., and Dou, S., 2017, "Recent Progress in Graphite Intercalation Compounds for Rechargeable Metal (Li, Na, K, Al)-Ion Batteries," *Adv. Sci.*, **4**(10), p. 1700146.
- [55] Cogswell, D. A., and Bazant, M. Z., 2012, "Coherency Strain and the Kinetics of Phase Separation in LiFePO<sub>4</sub> Nanoparticles," *ACS Nano*, **6**(3), pp. 2215–2225.
- [56] Schofield, P., Luo, Y., Zhang, D., Santos, D., Zaheer, W., Agbaworvi, G., Handy, J., Andrews, J., Braham, E., Balakrishna, A. R., and Banerjee, S., 2022, "Doping-Induced Pre-Transformation to Extend Solid-Solution Regimes in Li-Ion Batteries," *ACS Energy Letters*.
- [57] Markus, I. M., Lin, F., Kam, K. C., Asta, M., and Doeff, M. M., 2014, "Computational and Experimental Investigation of Ti Substitution in

Li<sub>1</sub>(Ni<sub>x</sub>Mn<sub>1-x</sub>Co<sub>(1-2x-y)</sub>Ti<sub>y</sub>)O<sub>2</sub> for Lithium Ion Batteries,” *J. Phys. Chem. Lett.*, **5**(21), pp. 3649–3655.

[58] Luo, Y., Rezaei, S., Santos, D. A., Zhang, Y., Handy, J. V., Carrillo, L., Schultz, B. J., Gobatto, L., Puppevski, M., Wiaderek, K., et al. et al., 2022, “Cation Reordering Instead of Phase Transitions: Origins and Implications of Contrasting Lithiation Mechanisms in 1D ζ- and 2D α-V<sub>2</sub>O<sub>5</sub>,” *Proc. Natl. Acad. Sci. U. S. A.*, **119**(4), p. e2115072119.

[59] Lee, E., Kwon, B. J., Dogan, F., Ren, Y., Croy, J. R., and Thackeray, M. M., 2019, “Lithiated Spinel LiCo<sub>1-x</sub>Al<sub>x</sub>O<sub>2</sub> As a Stable Zero-Strain Cathode,” *ACS Appl. Energy Mater.*, **2**(9), pp. 6170–6175.

[60] Oh, P., Yun, J., Park, S., Nam, G., Liu, M., and Cho, J., 2021, “Recent Advances and Prospects of Atomic Substitution on Layered Positive Materials for Lithium-Ion Battery,” *Adv. Energy Mater.*, **11**(15), p. 2003197.

[61] Yang, Y., Huang, J., Cao, Z., Lv, Z., Wu, D., Wen, Z., Meng, W., Zeng, J., Li, C. C., and Zhao, J., 2021, “Synchronous Manipulation of Ion and Electron Transfer in Wadsley–Roth Phase Ti–Nb Oxides for Fast-Charging Lithium-Ion Batteries,” *Adv. Sci.*, **9**, p. 2104530.

[62] Kolli, S. K., Natarajan, A. R., and Van der Ven, A., 2021, “Six New Transformation Pathways Connecting Simple Crystal Structures and Common Intermetallic Crystal Structures,” *Acta Mater.*, **221**, p. 117429.

[63] Kaufman, J. L., Vinčevićuće, J., Kolli, S. K., Giori, J. G., and Van der Ven, A., 2019, “Understanding Intercalation Compounds for Sodium-Ion Batteries and Beyond,” *Philos. Trans. R. Soc. A*, **377**(2152), p. 2019020.

[64] Tabor, D. P., Roch, L. M., Saikin, S. K., Kreisbeck, C., Sheberla, D., Montoya, J. H., Dwaraknath, S., Aykol, M., Ortiz, C., Tribukait, H., et al., 2018, “Accelerating the Discovery of Materials for Clean Energy in the Era of Smart Automation,” *Nat. Rev. Mater.*, **3**(5), pp. 5–20.

[65] Saal, J. E., Kirklin, S., Aykol, M., Meredig, B., and Wolverton, C., 2013, “Materials Design and Discovery With High-Throughput Density Functional Theory: The Open Quantum Materials Database (OQMD),” *JOM*, **65**(11), pp. 1501–1509.

[66] Zagorac, D., Müller, H., Ruehl, S., Zagorac, J., and Rehme, S., 2019, “Recent Developments in the Inorganic Crystal Structure Database: Theoretical Crystal Structure Data and Related Features,” *J. Appl. Crystallogr.*, **52**(5), pp. 918–925.

[67] Meng, Y. S., and Arroyo-de Dompablo, M. E., 2013, “Recent Advances in First Principles Computational Research of Cathode Materials for Lithium-Ion Batteries,” *Acc. Chem. Res.*, **46**(5), pp. 1171–1180.

[68] Chen, H., Hautier, G., Jain, A., Moore, C., Kang, B., Doe, R., Wu, L., Zhu, Y., Tang, Y., and Ceder, G., 2012, “Carbonophosphates: A New Family of Cathode Materials for Li-Ion Batteries Identified Computationally,” *Chem. Mater.*, **24**(11), pp. 2009–2016.

[69] Zhang, D., and Balakrishna, A. R., “Designing Shape-Memory-Like Microstructures in Intercalation Materials,” Under review, 2022.

[70] Lim, J., Li, Y., Alsem, D. H., So, H., Lee, S. C., Bai, P., Cogswell, D. A., Liu, X., Jin, N., Yu, Y.-S., et al., 2016, “Origin and Hysteresis of Lithium Compositional Spatiodynamics Within Battery Primary Particles,” *Science*, **353**(6299), pp. 566–571.

[71] Santos, D. A., Andrews, J. L., Bai, Y., Stein, P., Luo, Y., Zhang, Y., Pharr, M., Xu, B.-X., and Banerjee, S., 2020, “Bending Good Beats Breaking Bad: Phase Separation Patterns in Individual Cathode Particles Upon Lithiation and Delithiation,” *Mater. Horizons*, **7**(12), pp. 3275–3290.

[72] Ohmer, N., Fenk, B., Samuelis, D., Chen, C.-C., Maier, J., Weigand, M., Goering, E., and Schütz, G., 2015, “Phase Evolution in Single-Crystalline LiFePO<sub>4</sub> Followed by In Situ Scanning X-ray Microscopy of a Micrometre-Sized Battery,” *Nat. Commun.*, **6**(1), pp. 1–7.

[73] Li, Y., Gabaly, F. E., Ferguson, T. R., Smith, R. B., Bartelt, N. C., Sugar, J. D., Fenton, K. R., Cogswell, D., Kilcoyne, A. L., Tylliszczak, T., et al., 2014, “Current-Induced Transition From Particle-by-Particle to Concurrent Intercalation in Phase-Separating Battery Electrodes,” *Nat. Mater.*, **13**(12), pp. 1149–1156.

[74] Zhang, Y., and Tang, M., 2020, “Stress-Induced Intercalation Instability,” *Acta Mater.*, **201**, pp. 158–166.

[75] Mistry, A., Smith, K., and Mukherjee, P. P., 2020, “Stochasticity at Scales Leads to Lithium Intercalation Cascade,” *ACS Appl. Mater. Interfaces*, **12**(14), pp. 16359–16366.

[76] Cho, S., Chen, C.-F., and Mukherjee, P. P., 2015, “Influence of Microstructure on Impedance Response in Intercalation Electrodes,” *J. Electrochem. Soc.*, **162**(7), p. A1202.

[77] Chen, C.-F., and Mukherjee, P. P., 2015, “Probing the Morphological Influence on Solid Electrolyte Interphase and Impedance Response in Intercalation Electrodes,” *Phys. Chem. Chem. Phys.*, **17**(15), pp. 9812–9827.

[78] Chu, C., and James, R. D., 1995, “Analysis of Microstructures in Cu-14.0% Al-3.9% Ni by Energy Minimization,” *J. Phys. IV*, **5**(C8), pp. V8–143.

[79] Bai, P., Cogswell, D. A., and Bazant, M. Z., 2011, “Suppression of Phase Separation in LiFePO<sub>4</sub> Nanoparticles During Battery Discharge,” *Nano Lett.*, **11**(11), pp. 4890–4896.

[80] Ryu, H.-H., Park, K.-J., Yoon, C. S., and Sun, Y.-K., 2018, “Capacity Fading of Ni-Rich Li[Ni<sub>x</sub>Co<sub>1-x-y</sub>Mn<sub>(1-x-y)</sub>]O<sub>2</sub> (0.6 ≤ x ≤ 0.95) Cathodes for High-Energy-Density Lithium-Ion Batteries: Bulk Or Surface Degradation?,” *Chem. Mater.*, **30**(3), pp. 1155–1163.

[81] Xu, Z., Rahman, M. M., Mu, L., Liu, Y., and Lin, F., 2018, “Chemomechanical Behaviors of Layered Cathode Materials in Alkali Metal Ion Batteries,” *J. Mater. Chem. A*, **6**(44), pp. 21859–21884.

[82] Ebner, M., Marone, F., Stamparoni, M., and Wood, V., 2013, “Visualization and Quantification of Electrochemical and Mechanical Degradation in Li Ion Batteries,” *Science*, **342**(6159), pp. 716–720.

[83] Woodford, W. H., Chiang, Y.-M., and Carter, W. C., 2010, ““Electrochemical Shock” of Intercalation Electrodes: A Fracture Mechanics Analysis,” *J. Electrochem. Soc.*, **157**(10), p. A1052.

[84] Cogswell, D. A., and Bazant, M. Z., 2018, “Size-Dependent Phase Morphologies in LiFePO<sub>4</sub> Battery Particles,” *Electrochem. Commun.*, **95**, pp. 33–37.

[85] Andrews, J. L., Stein, P., Santos, D. A., Chalker, C. J., De Jesus, L. R., Davidson, R. D., Gross, M. A., Pharr, M., Batteas, J. D., Xu, B.-X., et al., 2020, “Curvature-Induced Modification of Mechano-Electrochemical Coupling and Nucleation Kinetics in a Cathode Material,” *Matter*, **3**(5), pp. 1754–1773.

[86] Ericksen, J. L., 2008, “On the Cauchy–Born Rule,” *Math. Mech. Solids*, **13**(3–4), pp. 199–220.

[87] Wang, Q., Zhang, G., Li, Y., Hong, Z., Wang, D., and Shi, S., 2020, “Application of Phase-Field Method in Rechargeable Batteries,” *npj Comput. Mater.*, **6**(1), pp. 1–8.

[88] Tang, M., Belak, J. F., and Dorr, M. R., 2011, “Anisotropic Phase Boundary Morphology in Nanoscale Olivine Electrode Particles,” *J. Phys. Chem. C*, **115**(11), pp. 4922–4926.

[89] Singh, G. K., Ceder, G., and Bazant, M. Z., 2008, “Intercalation Dynamics in Rechargeable Battery Materials: General Theory and Phase-Transformation Waves in LiFePO<sub>4</sub>,” *Electrochim. Acta*, **53**(26), pp. 7599–7613.

[90] Zhang, T., and Kamlah, M., 2020, “Mechanically Coupled Phase-Field Modeling of Microstructure Evolution in Sodium Ion Batteries Particles of Na<sub>2</sub>FePO<sub>4</sub>,” *J. Electrochem. Soc.*, **167**(2), p. 020508.

[91] Balakrishna, A. R., and Carter, W. C., 2018, “Combining Phase-Field Crystal Methods With a Cahn–Hilliard Model for Binary Alloys,” *Phys. Rev. E*, **97**(4), p. 043304.

[92] Balakrishna, A. R., Chiang, Y.-M., and Carter, W. C., 2019, “Phase-Field Model for Diffusion-Induced Grain Boundary Migration: An Application to Battery Electrodes,” *Phys. Rev. Mater.*, **3**(6), p. 065404.

[93] Hong, Y.-S., Huang, X., Wei, C., Wang, J., Zhang, J.-N., Yan, H., Chu, Y. S., Pianetta, P., Xiao, R., Yu, X., et al., 2020, “Hierarchical Defect Engineering for LiCoO<sub>2</sub> Through Low-Solubility Trace Element Doping,” *Chem*, **6**(10), pp. 2759–2769.

[94] Singer, A., Zhang, M., Hy, S., Cela, D., Fang, C., Wynn, T. A., Qiu, B., Xia, Y., Liu, Z., Ulvestad, A., et al., 2018, “Nucleation of Dislocations and Their Dynamics in Layered Oxide Cathode Materials During Battery Charging,” *Nat. Energy*, **3**(8), pp. 641–647.

[95] Nie, A., Gan, L.-Y., Cheng, Y., Li, Q., Yuan, Y., Mashayek, F., Wang, H., Klie, R., Schwingschlogl, U., and Shabbazian-Yassar, R., 2015, “Twin Boundary-Assisted Lithium Ion Transport,” *Nano Lett.*, **15**(1), pp. 610–615.

[96] Qian, G., Zhang, Y., Li, L., Zhang, R., Xu, J., Cheng, Z., Xie, S., Wang, H., Rao, Q., He, Y., et al., 2020, “Single-Crystal Nickel-Rich Layered-Oxide Battery Cathode Materials: Synthesis, Electrochemistry, and Intra-granular Fracture,” *Energy Storage Mater.*, **27**, pp. 140–149.

[97] Yan, P., Zheng, J., Gu, M., Xiao, J., Zhang, J.-G., and Wang, C. M., 2017, “Intragranular Cracking As a Critical Barrier for High-Voltage Usage of Layer-Structured Cathode for Lithium-Ion Batteries,” *Nat. Commun.*, **8**(1), pp. 1–9.

[98] Wang, R., Chen, X., Huang, Z., Yang, J., Liu, F., Chu, M., Liu, T., Wang, C., Zhu, W., Li, S., et al., 2021, “Twin Boundary Defect Engineering Improves Lithium-Ion Diffusion for Fast-Charging Spinel Cathode Materials,” *Nat. Commun.*, **12**(1), pp. 1–10.

[99] Besli, M. M., Xia, S., Kuppen, S., Huang, Y., Metzger, M., Shukla, A. K., Schneider, G., Hellstrom, S., Christensen, J., Doeff, M. M., et al., 2018, “Mesoscale Chemomechanical Interplay of the LiNi<sub>0.8</sub>Co<sub>0.15</sub>Al<sub>0.05</sub>O<sub>2</sub> Cathode in Solid-State Polymer Batteries,” *Chem. Mater.*, **31**(2), pp. 491–501.

[100] Kim, J. C., Seo, D.-H., Chen, H., and Ceder, G., 2015, “The Effect of Antisite Disorder and Particle Size on Li Intercalation Kinetics in Monoclinic LiMnBO<sub>3</sub>,” *Adv. Energy Mater.*, **5**(8), p. 1401916.

[101] Rasool, M., Chiu, H.-C., Lu, X., Voisard, F., Gauvin, R., Jiang, D.-T., Paoletta, A., Zaghbi, K., and Demopoulos, G. P., 2019, “Mechanochemically Tuned Structural Annealing: A New Pathway to Enhancing Li-Ion Intercalation Activity in Nanosized β II Li<sub>2</sub>FeSiO<sub>4</sub>,” *J. Mater. Chem. A*, **7**(22), pp. 13705–13713.

[102] Kang, B., and Ceder, G., 2009, “Battery Materials for Ultrafast Charging and Discharging,” *Nature*, **458**(7235), pp. 190–193.

[103] Kayyar, A., Qian, H., and Luo, J., 2009, “Surface Adsorption and Disorder in LiFePO<sub>4</sub> Based Battery Cathodes,” *Appl. Phys. Lett.*, **95**(22), p. 221905.

[104] Tang, M., Carter, W. C., and Chiang, Y.-M., 2010, “Electrochemically Driven Phase Transitions in Insertion Electrodes for Lithium-Ion Batteries: Examples in Lithium Metal Phosphate Olivines,” *Annu. Rev. Mater. Res.*, **40**, pp. 501–529.

[105] Luo, J., 2019, “Let Thermodynamics Do the Interfacial Engineering of Batteries and Solid Electrolytes,” *Energy Storage Mater.*, **21**, pp. 50–60.

[106] Yan, Q., Ko, S. T., Dawson, A., Agyeman-Budu, D., Whang, G., Zhao, Y., Qin, M., Dunn, B. S., Weker, J. N., Tolbert, S. H., et al., 2022, “Thermodynamics-Driven Interfacial Engineering of Alloy-Type Anode Materials,” *Cell Rep. Phys. Sci.*, **3**(1), p. 100694.

[107] Cantwell, P. R., Frollov, T., Rupert, T. J., Krause, A. R., Marvel, C. J., Rohrer, G. S., Rickman, J. M., and Harmer, M. P., 2020, “Grain Boundary Complexion Transitions,” *Annu. Rev. Mater. Res.*, **50**, pp. 465–492.